

***K*-shell ionization cross sections for targets from $Z = 21$ to $Z = 47$ induced by He ions and by protons in the energy range 0.2–2.5 MeV/u**

Donald G. Simons,* Jack L. Price, David J. Land, and Matt D. Brown

Naval Surface Warfare Center, Silver Spring, Maryland 20903-5000

(Received 23 September 1988)

Absolute *K*-shell x-ray production cross sections have been measured for ${}^3\text{He}$ ions in the energy range from 0.175 to 1.6 MeV/u incident on selected thin-foil targets from Ti ($Z = 22$) through Ag ($Z = 47$). A few measurements were made for incident ${}^4\text{He}$ ions at energies from 0.2 to 0.6 MeV/u in order to study the effects of Coulomb deflection and retardation. Newly measured values are also reported for incident protons at energies from 0.5 to 2.5 MeV on numerous target elements from Sc ($Z = 21$) through Zn ($Z = 30$). The x-ray production cross sections were determined from x-ray yields normalized to simultaneous measurements of particle-scattering yields at 75° . The *K*-shell ionization cross sections inferred from these results are compared with the predictions of the energy-loss Coulomb-deflection perturbed-stationary-state relativistic theory. There is agreement generally to within 10% although a systematic discrepancy, previously observed, is reproduced. Close agreement is obtained for protons with the reference values of Paul and Muhr [Phys. Rep. **135**, 47 (1986)]. This investigation is part of an overall experimental-theoretical program whose goals are (1) to enlarge the data base of ion-induced x-ray production cross sections by establishing accurate experimental values and (2) to determine the limitations of the current theoretical descriptions of the inner-shell ionization process and their ability to calculate experimental quantities precisely.

I. INTRODUCTION

The problem of the inner-shell ionization of heavy atoms by energetic positive ions through the direct Coulomb interaction continues to challenge current theoretical models for accurate predictive capability of total and differential cross sections.^{1–3} Asymmetric collision systems are assumed, i.e., systems for which the inequality $Z_1/Z_2 \leq 0.3$ is satisfied, where Z_1 and Z_2 are the atomic numbers of the projectile ion and target atom, respectively. A critical parameter, the reduced velocity $\xi = \hbar v / (E_B r_s)$, defines physically distinct regimes.^{4,5} Here v is the projectile velocity, E_B the binding energy of the inner-shell electron, and r_s the radius of the atomic shell which, for the *K* shell, is a_0/Z_{2K} , with a_0 the Bohr radius and $Z_{2K} = Z_2 - 0.3$. For high-velocity collisions having $\xi \gg 1$, the target-electron wave function remains unperturbed by the passage of the projectile. In this regime the plane-wave Born approximation (PWBA) should be valid.⁶ At lower velocities with $\xi \leq 1$, the target electron responds to the presence of the projectile through a distortion or polarization of its wave function.⁵ The investigations reported here relate to the physically interesting low to moderate velocity region in ξ .

The present paper pertains to a combined experimental-theoretical effort whose goals are both to enlarge the data base of ion-induced x-ray production cross sections with accurate absolute values for application to materials analysis and to determine to what extent current theoretical description of inner-shell ionization enables precise calculation of experimentally accessible parameters. Our overall investigations to date have been concerned almost

exclusively with *K*-shell ionization cross sections, both total and differential in the projectile scattering angle, induced by protons and helium ions with reduced velocities in the range $0.2 < \xi < 1.2$ incident on selected targets with atomic numbers from Sc ($Z = 21$) through Ag ($Z = 47$). This paper deals with the experimental measurements of the total cross sections for helium and proton projectiles. Details of the work dealing with the experimental measurement of the differential cross sections and with the theoretical investigation are deferred to future publications.

In order to cover the broadest region in ξ for helium projectiles with the available accelerator facility, ${}^3\text{He}$ ions were chosen as projectiles. With ξ ranging from 0.22 to 0.96 we have established one of the largest data bases developed by a single experimental group for He projectiles in this velocity region. A few measurements were also made for ${}^4\text{He}$ projectiles in order to determine the ${}^4\text{He}$ to ${}^3\text{He}$ cross section ratio. This ratio relates to the effects of the Coulomb interaction between the projectile and target nucleus which induces a retardation and deflection of the projectile.

In a previous publication⁷ we reported measurements of the total cross section for *K*-shell ionization for incident protons in the energy region of 0.3 to 2.5 MeV. The present investigation involving He projectiles is similar with respect to target atoms and projectile velocities to the earlier one for incident protons. However, some details of the experimental arrangement were changed to allow for a more accurate determination of solid angles and beam alignment. Hence, new measurements of the proton cross sections were made and their results are also

reported here.

For values of $\xi \leq 1$ several specific physical phenomena are well known to influence the ionization cross sections profoundly. These include the change in the binding energy of the *K*-shell electron,^{4,8} the distortion or polarization of the electron wave function,⁵ and the influence of the hyperbolic Coulomb trajectory of the projectile.⁹ In one theoretical approach to this problem, these phenomena have been felicitously modeled and incorporated into the PWBA. This model has become widely labeled as ECPSSR,^{4,5,10,11} standing for the energy-loss Coulomb-deflection perturbed-stationary-state relativistic theory. The ionization cross sections predicted by this model correlate well with experimental values, not just for the *K* shell,¹² but for the *L* shell¹⁰ as well and, to some extent, for the *M* shell.¹³ This agreement holds for protons and helium particles and also for higher-*Z* projectiles¹⁴ over a wide range of incident energies and for targets from the entire periodic table.

A second approach to this problem, facilitated today by the availability of fast computers, is to solve directly the coupled channel equations that arise from substituting an expansion of the atomic wave function in terms of suitable basis states into the time-dependent Schrödinger equation.¹⁻³ There are available from the literature far fewer solutions for comparisons with data, but the indications are that the predicted cross sections tend to be low for incident protons¹ and even lower for incident helium ions.¹⁵ These solutions, however, do represent a fundamental approach to this problem.

A third strategy, midway between the two just described, is central to the present combined experimental-theoretical investigation. While based on lowest-order perturbation theory, it utilizes the freedom of the selection of basis states in the expansion of the total wave function. In particular, the response of the target electron to the presence of the charged projectile is modeled through the use of a suitably constructed, initial-state wave function which exhibits its expected distortion or polarization.^{16,17} In addition, the change in the electron binding energy due to the projectile is incorporated. These are both inherently time-dependent effects as they are a function of the location of the incident particle.¹⁸ An implementation of these ideas has been formulated in a time-independent framework in which all time-varying quantities are evaluated at a fixed projectile position such as the distance of closest approach to the target nucleus.^{18,19} The results of calculations for incident protons and ³He projectiles on Ti and ⁶Li projectiles²⁰ on Cr in the velocity region considered here show an increasingly larger discrepancy with experimental values as the charge of the projectile is increased. Recently these ideas have been formulated¹⁷ such that the electron binding energy and wave function are treated as time dependent with a hyperbolic Coulomb trajectory to describe the motion of the projectile, as prescribed by the basic tenets of the model. This model is termed PSS-C in this paper. The results of calculations for the systems studied here and for the corresponding systems with ⁶Li ions as projectiles confirm the discrepancy noted above. In particular, good agreement, to about 5%, is found for protons, with

15–20 % discrepancy for He and a 30–45 % discrepancy for Li. On the other hand, calculations based upon this theory agree with the results of calculations from close-coupled methods discussed above.^{1,15} We conclude that, while the basic physics of inner-shell ionization may be understood, additional physical interaction remains to be included to enable precise calculation of the process. As previously noted, details of this model will be given elsewhere.

II. EXPERIMENTAL PROCEDURE

Ionization cross sections were inferred from measurements of x-ray production cross sections and tabulated values of fluorescence yields. Experiments were performed on the Naval Surface Warfare Center 2.5-MV Van de Graaff positive-ion accelerator. The beam energy was determined by magnetic analysis with a 90° bending magnet and an NMR magnet control system. A beam energy resolution of 1–2 keV at 1000 keV was obtained through a combination of exit slit and capacitive pick-off feedback.

Measurements were made using the common procedure of simultaneous measurements of ion-induced x rays and of particles scattered into a fixed laboratory angle. By normalizing the counts in the x-ray detector to the number of simultaneously detected particles, beam currents are eliminated from consideration and the effects of target nonuniformities and inhomogeneities are considerably reduced. The x-ray detector and the particle detector were placed at 90° and 75° with respect to the direction of the incident beam, respectively. The total *K*-shell vacancy production cross section σ_v is thus given by

$$\sigma_v = \frac{N_x \left[\frac{d\sigma^R(\theta, E)}{d\Omega_p} \right] d\Omega_p}{N_p \omega_k \epsilon_x \frac{d\Omega_x}{4\pi}}, \quad (1)$$

where N_x and N_p are the x-ray and particle counts; $d\sigma^R(\theta, E)/d\Omega_p$ is the Rutherford scattering cross section for the incident particles scattered at the laboratory angle θ (75° here) and at the projectile energy E ; $d\Omega_x$ and $d\Omega_p$ are the x-ray and particle solid angles, respectively; ϵ_x the x-ray detector efficiency for the *K* x rays; and ω_k is the target fluorescence yield. The values for the total cross section given by Eq. (1) are corrected⁷ to account for the change in the x-ray production and Rutherford scattering cross sections arising from the finite thickness of the target. As is customary, it is assumed that the contribution to the vacancy production cross section from excited states is small so that σ_v is equivalent to the total *K*-shell ionization cross section.

The general experimental procedure has been reported previously⁷ in our work with proton inner-shell ionization measurements on targets of similar atomic number. Therefore we will only outline the differences in the experimental procedure and analysis here. In our previous

TABLE I. K-shell vacancy production cross sections induced by ^3He and ^4He ions as a function of energy in keV/u. Cross section values are given in barns. The values for the fluorescent yields are from Krause and are given for each element. The numbers in brackets denote power-of-ten factors.

Energy (keV/u)	Projectile ^3He		^3He		^3He		^3He		^3He		^3He		^4He		^4He	
	Target atom	Ti	Cr	Co	Cu	Ge	Zr	Ag	Ti	Cu	Ge	Ag	Ti	Cu	Ge	Ge
	Fluorescent yield	0.214	0.275	0.373	0.440	0.535	0.730	0.830	0.214	0.440	0.535	0.830	0.214	0.440	0.535	0.535
175	2.00		6.73[-1]		6.00[-2]				2.25	7.36[-2]			2.25	7.36[-2]		
200	3.15		1.20	3.00[-1]	1.13[-1]	3.38[-2]			3.85	1.50[-1]			3.85	1.50[-1]	4.65[-2]	
225	5.27		2.00		2.04[-1]				5.65	2.29[-1]			5.65	2.29[-1]		
250	7.55		2.85	8.20[-1]	3.30[-1]	1.02[-1]			8.56	3.91[-1]			8.56	3.91[-1]	1.28[-1]	
300	1.46[+1]		5.82	1.69	7.09[-1]	2.14[-1]			1.67[+1]	8.26[-1]			1.67[+1]	8.26[-1]	2.79[-1]	
350	2.58[+1]		1.02[+1]	3.13	1.30	4.32[-1]			2.94[+1]	1.50			2.94[+1]	1.50	5.15[-1]	
400	4.19[+1]		1.64[+1]	4.97	2.12	7.38[-1]			4.83[+1]	2.34			4.83[+1]	2.34	8.47[-1]	
500	8.90[+1]		3.61[+1]	1.06[+1]	4.81	1.69			9.76[+1]	5.15			9.76[+1]	5.15	1.93	
600	1.67[+2]		6.68[+1]	1.92[+1]	9.16	3.20			1.74[+2]	9.39			1.74[+2]	9.39	3.49	
700	2.75[+2]		1.09[+2]	3.29[+1]	1.55[+1]	5.52										
800	4.11[+2]		1.65[+2]	5.15[+1]	2.46[+1]	8.57										
900	5.85[+2]		2.43[+2]		3.58[+1]											
1000	7.87[+2]		3.42[+2]		4.90[+1]											
1100	9.96[+2]		4.20[+2]		6.71[+1]											
1200	1.31[+3]		5.73[+2]		8.48[+1]											
1300	1.54[+3]		6.87[+2]		1.09[+2]											
1400	1.90[+3]		8.24[+2]		1.32[+2]											
1500	2.16[+3]		9.76[+2]		1.53[+2]											
1600	2.47[+3]				1.89[+2]											

^aMeasurement made at 940 keV/u.

experimental arrangement, difficulties were encountered in the measurement of the detector solid angles and in beam alignment. The use of a larger scattering chamber in the present system allows a more accurate geometrical measurement of the solid angles, eliminating the need for corroborating measurements with calibrated radioactive sources. With respect to the beam alignment, it had not been possible to determine with sufficient precision that the beam and the target intersected at the center of the scattering chamber, even with the addition of a monitor particle detector. In the improved apparatus better alignment was achieved by the addition of a beam viewer at the center of the scattering chamber, and realignment of the beam was performed for every change of beam energy. Assurance of beam alignment was obtained by requiring that the ratio of counts between the monitor detector (now placed at 150°) and the 75° particle detector be equal to the ratio of product of the Rutherford scattering cross section and the solid angle of their respective detectors to within experimental error. The change in particle scattering angle from 90° to 75° also reduces the possibility of interference between the scattered beam and the target holder.

The sources of error are the same as in our previous work. We have taken into account errors from counting statistics (generally 1% but larger in some cases as mentioned below), solid angles for the x-ray detector (2%) and the particle detector (2%), x-ray detector efficiency (2%), beam energy (0.2% at high beam energies and 2% at low energies), and energy loss through the target (0.5% at high beam energies and 2% at low energies). The errors from these sources are essentially the same for proton and for the helium projectiles. The error in the Rutherford scattering cross section which is derived from the uncertainty in the scattering angle, however, depends on the projectile. For both cases it is estimated that the error in the scattering angle is 1° . At a scattering angle of 75° this uncertainty results in an error of 3% for protons and 7% for helium.

On accumulating the above errors in quadrature, the error for protons ranges from 4.7% to 5.5% for all targets except V, which is estimated to have an error of 10% because of poorer counting statistics. With the larger error in the Rutherford scattering cross section, the helium measurements are inherently less accurate than those for protons with errors ranging from 8.0% to 8.4% for all of the targets except Zr and Ag. In these two cases the errors in counting statistics are larger because of lower x-ray counts and larger backgrounds in the x-ray detector with the error for Zr increasing to 9% and for Ag to 11%.

III. RESULTS AND DISCUSSIONS

Total K-shell ionization cross sections were measured for ^3He and ^4He projectiles incident on targets of Ti, Cr, Ni, Cu, Ge, Zr, and Ag. The energy range was from 0.175 to 1.6 MeV/u for ^3He and from 0.175 to 0.6 MeV/u for ^4He . In order to cover the entire energy range for the ^3He projectiles both singly and doubly

charged ions were used; the ^4He projectiles were singly charged only. We also made new measurements of the proton cross sections at energies from 0.5 to 2.5 MeV. The targets studied were Sc, Ti, V, Cr, Co, Ni, Cu, and Zn. The resulting numerical values for the cross sections in barns are given in Table I for ^3He and ^4He and in Table II for incident protons. The fluorescence yields²¹ used in the data reduction are also listed.

The total cross sections inferred from these measurements are compared with those obtained from the ECPSSR theory of Brandt and Lapicki¹¹ by plotting the ratio of the experimental to the ECPSSR values as a function of the reduced velocity ξ of the incident projectile. The results of these comparisons are shown in Fig. 1 for the ^3He projectiles and in Fig. 2 for ^4He . A strong systematic variation in this ratio as a function of ξ is clearly seen in these figures. The shape and magnitude of the ratios of this comparison for ^3He agree closely with compilations of Paul and Muhr¹² for ^4He . The values of the cross sections induced by ^4He also agree with the values obtained by Lopes *et al.*²² for targets studied here and for other targets with similar atomic numbers. We see from the figure that for $0.4 < \xi < 1.0$ the ECPSSR values are generally larger than the experimental values with the ratios rising toward unity as ξ approaches unity. For values of $\xi < 0.4$ the ratio reverses itself and the ECPSSR values become smaller than the experimental values. There is some indication that the ratio reverses itself again as ξ becomes even smaller. This behavior is in agreement with other observations¹² and has been explained²³ in terms of the inadequacy of the Coulomb correction factor in the ECPSSR model at very low velocities ($\xi < 0.2$). From Fig. 1 we note that the width of the band of the ^3He values reflects the consistency of the experimental data with the uncertainty of 5% associated with the random error for all targets except Ag. For Ag (not plotted in Fig. 1) the ratio of the experimental values to the ECPSSR values is near unity throughout the entire

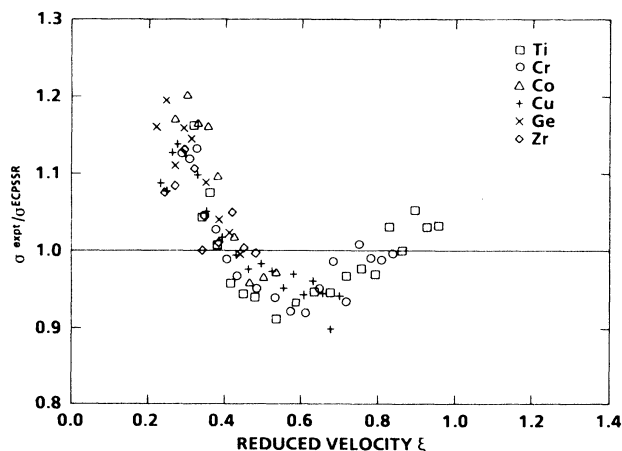


FIG. 1. Ratio of the present experimental values to the ECPSSR values of the total K-shell ionization cross sections for ^3He projectiles vs the reduced velocity $\xi = (\hbar v / E_B) / (a_0 / Z_{2K})$ for several targets.

TABLE II. Proton induced K -shell vacancy production cross sections as a function of energy. Cross section values are given in barns. The values of the fluorescent yields are from Krause and are given for each element.

Energy (keV)	Target atom Sc	Ti	V	Cr	Co	Ni	Cu	Zn
	Fluorescent yield 0.188	0.214	0.243	0.275	0.373	0.406	0.440	0.474
500	5.08[+1]	3.22[+1]					1.54	1.02
600	9.10[+1]	5.78[+1]			6.64		3.00	2.00
700	1.44[+2]	9.05[+1]			1.10[+1]		5.24	3.41
800	2.08[+2]	1.31[+2]		5.47[+1]	1.67[+1]		8.05	5.32
1000	3.65[+2]	2.28[+2]	1.70[+2]	1.01[+2]	3.29[+1]	2.21[+1]	1.57[+1]	1.11[+1]
1200	5.45[+2]	3.41[+2]	2.55[+2]	1.57[+2]	5.36[+1]	3.67[+1]	2.61[+1]	1.85[+1]
1400	7.47[+2]	4.77[+2]	3.46[+2]	2.25[+2]	7.84[+1]	5.55[+1]	3.95[+1]	2.85[+1]
1600	9.31[+2]	6.16[+2]	4.47[+2]	3.02[+2]	1.09[+2]	7.70[+1]	5.55[+1]	4.06[+1]
1800	1.09[+3]	7.70[+2]	5.55[+2]	3.93[+2]	1.42[+2]	1.04[+2]	7.38[+1]	5.38[+1]
2000	1.29[+3]	9.21[+2]	7.04[+2]	4.66[+2]	1.77[+2]	1.28[+2]	9.43[+1]	6.89[+1]
2200	1.51[+3]	1.05[+3]	7.76[+2]	5.40[+2]	2.14[+2]	1.55[+2]	1.15[+2]	8.56[+1]
2300	1.63[+3]	1.16[+3]		5.86[+2]			1.30[+2]	
2400	1.67[+3]	1.22[+3]		6.25[+2]			1.44[+2]	
2500	1.73[+3]	1.29[+3]		6.49[+2]			1.53[+2]	

range of reduced velocity. This result is consistent with the compilations of Paul and Muhr¹² for targets with atomic numbers in the range between 40 to 50.

In Fig. 3 we show a comparison of the results of the measured cross sections for incident protons with the reference cross sections of Paul and Muhr.¹² Close agreement, to within 5%, is noted except for the V ($Z=23$) data to which a 10% uncertainty was assigned.

In the comparison of measurements involving ^3He and ^4He projectiles the difference in the cross sections at equal incident velocity should arise from the slowing down and deflection of the projectile brought about by Coulomb interaction between it and the target nucleus, since the only difference between the two projectiles is the mass. In Fig. 4 the ratios of the measured values of ^4He to ^3He as a function of energy per atomic mass unit for targets of Ti, Cu, and Ge are shown. Also shown are ra-

tios from the two theoretical models discussed above, ECPSSR and PSS-C. The error associated with the experimental points in the figure results from propagating the 5% random errors associated with the data to yield a net error of 7% in the ratio. It has been assumed that the systematic errors would cancel. Most of the data points fall within one standard deviation of the theoretical curves though the data generally lie above the curves. The reason for this systematic difference is not clear. Nevertheless, the results of the experimental measurements are sufficiently accurate so as to confirm the general trends of the theoretical predictions relating to Coulomb effects. The ratios from the PSS-C (Ref. 17) theory which incorporates a rigorous hyperbolic Coulomb trajectory are slightly closer to the experimental values, particularly for Ge. The apparent change in

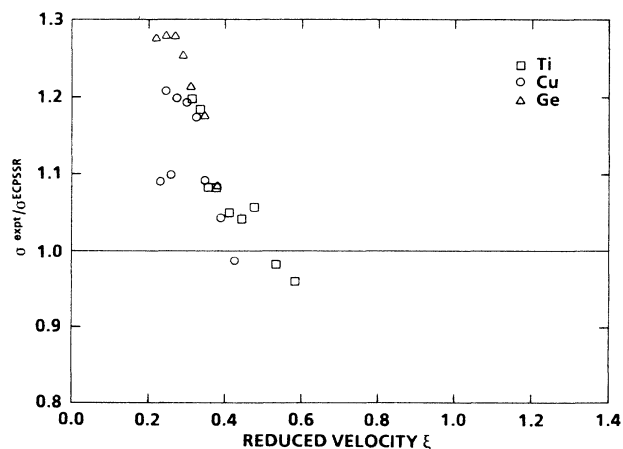


FIG. 2. Ratio of the present experimental values to the ECPSSR values of the total K -shell ionization cross sections for ^4He projectiles vs ξ for several targets.

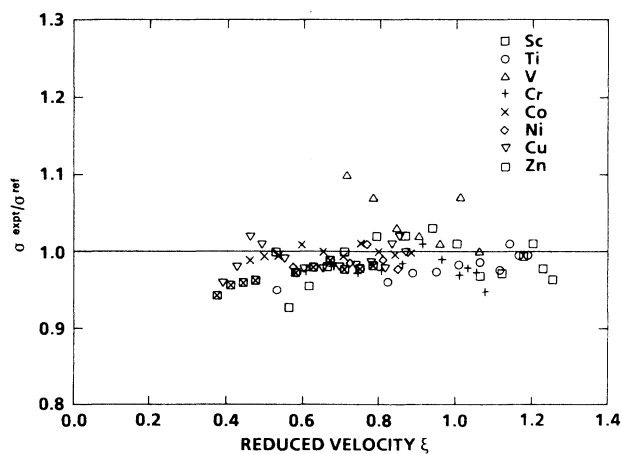


FIG. 3. Ratio of the present experimental values to the reference values of Paul and Muhr (Ref. 12) for the total K -shell ionization cross sections for incident protons vs ξ for several targets.

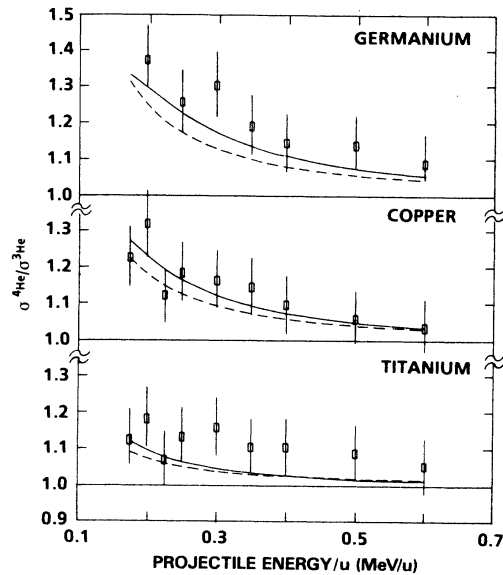


FIG. 4. Ratio of the total K -shell ionization cross sections for ${}^4\text{He}$ to ${}^3\text{He}$ projectiles vs projectile energy for Ti, Cu, and Ge targets. In the figure the rectangles with error bars represent the experimental data, the dashed curves the ECPSSR values, and the solid curves the PSS-C values.

curvature of the PSS-C curve for Ge at the lower energies is a direct result of the increasing importance of the P -wave final-state contribution to the amplitude at low velocities when a Coulomb trajectory is used. It arises from

the overlap of the projectile with the lobes of the $m = \pm 1$ final-state amplitudes and is associated with the deflection of the projectile rather than from its slowing down.

IV. CONCLUSIONS

We have presented here experimentally determined values for the total K -shell ionization cross section for ${}^3\text{He}$ and ${}^4\text{He}$ ions and protons on selected targets from Sc through Ag in the velocity region $0.2 < \xi < 1.2$. The ${}^3\text{He}$ measurements are the only ones for this projectile on the targets considered and represent one of the largest data bases for He projectiles measured by a single group in the low-velocity regime of $\xi \leq 1$. The experimental values are generally close to those found by other groups for both He ions and protons. The theoretical values of the ratios of the ${}^4\text{He}$ to ${}^3\text{He}$ cross sections, while systematically lower than corresponding experimental values, lie within the experimental uncertainty, particularly in the case of the PSS-C theory.

ACKNOWLEDGMENTS

The authors wish to thank Professor Helmut Paul of the University of Linz for a careful reading of the manuscript and for some helpful comments. They also thank Mr. Patrick K. Cady for his tireless efforts in accelerator maintenance and data acquisition. This investigation was supported by the Independent Research Program of the Naval Surface Warfare Center.

*Present address: Catholic University of America, Washington, D.C. 20064.

¹A. L. Ford, E. Fitchard, and J. F. Reading, *Phys. Rev. A* **16**, 133 (1977).

²W. Fritsch and C. D. Lin, *Phys. Rev. A* **29**, 2395 (1984); T. G. Winter and C. D. Lin, *ibid.* **29**, 3071 (1984).

³G. Mehler, W. Greiner, and G. Soff, *J. Phys. B* **20**, 2787 (1987).

⁴G. Basbas, W. Brandt, and R. Laubert, *Phys. Rev. A* **7**, 983 (1973).

⁵G. Basbas, W. Brandt, and R. Laubert, *Phys. Rev. A* **17**, 1655 (1978).

⁶E. Merzbacher and H. W. Lewis, *Corpuscles and Radiation in Matter II*, Vol. 34 of *Handbuch der Physik*, edited by S. Flügge (Springer-Verlag, Berlin, 1958), p. 166.

⁷M. D. Brown, D. G. Simons, D. J. Land, and J. G. Brennan, *Phys. Rev. A* **25**, 2935 (1982).

⁸W. Brandt, R. Laubert, and I. Sellin, *Phys. Rev.* **151**, 56 (1966).

⁹O. Aashamar and L. Kocbach, *Z. Phys. A* **279**, 237 (1976); *J. Phys. B* **10**, 869 (1977); G. L. Swafford, J. F. Reading, A. L. Ford, and E. Fitchard, *Phys. Rev. A* **16**, 1329 (1977).

¹⁰W. Brandt and G. Lapicki, *Phys. Rev. A* **20**, 465 (1979).

¹¹W. Brandt and G. Lapicki, *Phys. Rev. A* **23**, 1717 (1981).

¹²H. Paul and J. Muhr, *Phys. Rep.* **135**, 47 (1986).

¹³R. Metha, J. L. Duggan, J. L. Price, F. D. McDaniel, and G. Lapicki, *Phys. Rev. A* **26**, 1883 (1982); **28**, 1189(E) (1983); R. Metha, J. L. Duggan, J. L. Price, P. M. Kocur, F. D. McDaniel, and G. Lapicki, *ibid.* **28**, 3217 (1983).

¹⁴M. C. Andrews, F. D. McDaniel, J. L. Duggan, P. D. Miller, P. L. Pepmiller, H. F. Krause, T. M. Rosseel, L. A. Rayburn, R. Metha, and G. Lapicki, *Nucl. Instrum. Meth.* **B10/11**, 186 (1985); J. L. Price, J. L. Duggan, F. D. McDaniel, G. Lapicki, and R. Metha, *Phys. Rev. A* **32**, 2088 (1986).

¹⁵H. Paul (private communication).

¹⁶G. Basbas and D. J. Land, *Phys. Rev. A* **35**, 1003 (1987).

¹⁷D. J. Land, *Bull. Amer. Phys. Soc.* **33**, 1005 (1988); *Nucl. Instrum. Meth.* **B24/25**, 252 (1987).

¹⁸G. Basbas, W. Brandt, and R. H. Ritchie, *Phys. Rev. A* **7**, 1971 (1973).

¹⁹D. J. Land, *Nucl. Instrum. Meth.* **A240**, 470 (1985).

²⁰B. Raith, S. Divoux, and B. Gonsior, *Nucl. Instrum. Meth.* **B10/11**, 169 (1985).

²¹M. O. Krause, *J. Phys. Chem. Ref. Data* **8**, 307 (1979).

²²J. S. Lopes, A. P. Jesus, and M. F. da Silva, *J. Phys. B* **15**, 1749 (1982).

²³H. Paul, *Nucl. Instrum. Meth.* **B4**, 211 (1984).